

General Disclaimer

One or more of the Following Statements may affect this Document

- This document has been reproduced from the best copy furnished by the organizational source. It is being released in the interest of making available as much information as possible.
- This document may contain data, which exceeds the sheet parameters. It was furnished in this condition by the organizational source and is the best copy available.
- This document may contain tone-on-tone or color graphs, charts and/or pictures, which have been reproduced in black and white.
- This document is paginated as submitted by the original source.
- Portions of this document are not fully legible due to the historical nature of some of the material. However, it is the best reproduction available from the original submission.

Contract 956292

9950 - 696

Maser Radiometer for Cosmic Background Radiation

Anisotropy Measurements

FINAL REPORT

by

Dale J. Fixsen

and

David T. Wilkinson

Physics Department
Princeton University
Princeton, New Jersey
08544



Prepared for

The Jet Propulsion Laboratory
California Institute of Technology

June, 1982

(NASA-CR-169212) MASER RADIOMETER FOR
COSMIC BACKGROUND RADIATION ANISOTROPY
MEASUREMENTS Final Report (Princeton Univ.,
N. J.) 13 p HC A02/MF A01

CSCL 20E

N82-30538

Unclass

G3/36 28597

SUMMARY

A maser amplifier, built at JPL, has been incorporated into a low-noise radiometer designed to measure large-scale anisotropy in the 3°K microwave background radiation. To minimize emission by atmospheric water vapor and oxygen, the radiometer is flown in a small balloon to an altitude of 25 km. Three successful flights have been made - two from Palestine, Texas and one from Sao Jose dos Campos, Brazil. Good sky coverage is important to the experiment.

Data from the northern hemisphere flights has been edited and calibrated, and a copy sent to S. Gulkis at JPL. Analysis of the data is currently under way at Princeton University.

I. Radiometric System

The maser-based radiometer system is shown in Figure 1. Below, the various important components of this system are discussed, with special emphasis on the maser.

1. Maser

The 4-stage reflected wave maser used in this experiment was designed by Robert Claus (JPL) and Craig Moore (NRAO). One stage of the maser consists of ruby-filled waveguide (see Fig. 2) with a three-port circulator at one end and a reflector at the other end. This arrangement enables the wave to pass through the ruby twice. To avoid oscillation the gain of a single stage must be limited to about 10. Four stages are required to produce sufficient gain to minimize the noise of the following receiver. The four stages are "stacked" to place the four rubies in the magnetic field of a superconducting magnet. There are additional circulators between the stages with loads on the third port to absorb waves going backwards, since

unavoidable reflections would allow backward waves to contribute noise. At the circulators the microwaves propagate in the direction indicated by the arrows. The microwaves propagate down the ruby and are reflected off the end and propagate back up with a gain of about 9 dB. The electronic gain through the 4 rubies is 36 dB, but the losses in the walls and circulators reduce this to about 30 dB of net gain.

To obtain a 400 MHz bandwidth the magnetic field is tapered along the length of the ruby. (8800 to 8950 gauss in 15 cm), so different parts of the ruby amplify different frequencies. The field taper is obtained by making the magnetic pole pieces closer together at the bottom than at the top. By changing the taper, gain can be traded for bandwidth and vice-versa.

The pump frequency required is $2f+3$ GHz for maser frequencies between 10 and 35 GHz, and the bandwidth must be twice the maser bandwidth. Thus the pump must be a broad-band source or sweep across the band in a time short compared with the spin relaxation time, which is 30 ms. The pump frequency was swept across the band at 10 kHz.

Providing enough pump power to saturate the pumped transitions over a 1 GHz band proved to be a problem. The relaxation time implies a power consumption of about 15 mW. The pump source, an electronically tunable Gunn diode (51.4 to 52.4 GHz), produces about 70 mW. This is reduced to 50 mW by losses in the wave guide to the maser. The short wavelength pump power enters the bottom of the maser (see Fig. 2) through waveguide which is too small to pass the maser frequency. There is a discontinuity at the interface between the two sizes of wave guide which has a frequency dependent reflection. It was determined experimentally that about 1/6 of the remaining power is absorbed by the ruby. The rest of the power continues through the ruby and is absorbed by the loads at the top of the maser.

The low pump power absorption reduces the maser gain and makes the gain a strong function of pump power (1 dB increase in pump power results in 2 dB increase in gain). The output power of the pump oscillator depends on frequency and temperature. This is the dominating instability in the maser.

There are several problems which result in gain ripple (gain variation as a function of frequency). One of the major problems is internal reflections. The ruby has a dielectric constant of about 10. The wave guide is reduced to 1/3 normal size (in both dimensions) to limit the 24.6 GHz waves to a single mode. A stepped transition in conjunction with a 17 mm taper on a ruby limit the power reflection to about 5%. The circulators have a reflection of about 1%. These two reflections limit the gain of the one stage of the maser to about 10 since if the gain times the reflection exceeds unity the maser is unstable.

End effects of the magnet also introduce gain ripple. The magnet pole pieces have superconductors on the sides to keep the field uniform across the face. However at the ends of the magnet, the field spreads and lowers the magnetic field. This condition was corrected by inserting a tapered iron shim between the maser and the pole face.

There are several ways the ripple might be reduced. A longer magnet would solve the end-effects problem. Making the ruby without a taper (or using some inactive dielectric for the taper) would make the shimming problem somewhat more tractable. A more powerful pump would reduce some ripple caused by the frequency-dependent output of the pump (and the reflections) as well as stabilize the maser. Small coils could be placed on the face of the magnet allowing dynamic tuning of the maser.

The gain is a very strong function of temperature. The gain depends on the exponential of the inversion, which in turn has an exponential

dependence on the temperature. To maintain a constant temperature the maser is cooled by boiling liquid helium. The boiling point of liquid helium is a function of the pressure, so during the flight the pressure is maintained, at 1 atm, by a simple diaphragm regulator. In addition, the pressure and temperature are monitored throughout the flight. The pressure remained constant to 1% over the flight (the sensor limits the measurement accuracy), a 1% decrease in the pressure would lead to a 10% increase in the gain.

An external magnetic field was applied to the dewar to determine the effects the earth's magnetic field would have on the maser. The gain of the maser changed about 2%/gauss when a field was applied to the pump or to the dewar containing the maser. After shielding the pump and coating the surface of the maser shield with lead, a superconductor at 4 K, there remained an effect of about .2%/gauss. To stop the field lines from entering the top of the can a magnetic shunt, consisting of two parallel bars (each 4 mm x 10 mm x 120 mm) of cold rolled steel, was placed across the top of the shield. The remaining residual effect was measured at about .05%/gauss.

In summary, the maser has an effective gain of 1000 and an effective bandwidth of 300 MHz. The predicted noise was 6 K which agrees with the measured value of 6 ± 2 K. The amplification becomes non-linear (1 dB compression point) when the input is 6×10^8 K, giving the maser 80 dB of dynamic range.

2. Horns

The circular corrugated horns are 43 cm long and with a 16 cm aperture. Grooves are cut at 3/8 wave intervals, one quarter wave deep, in the aluminum walls of the horns. These corrugations reduce side-lobe response and using the measured horn pattern (see Fig. 3) the total ground radiation the horn

receives is estimated at .4 mK. Radiation from the walls of the horns is estimated at 3 K.

3. Couplers and Windows

Bethe hole couplers insert a calibrated signal into the system to provide in-flight calibration. The source is a broad band noise diode which is stable over a wide temperature range (5% variation 77 K to 300 K). The 42 and 47 dB couplers add 6.2 K and 1.2 K respectively when the diodes are turned on. Losses in the transitions and couplers add 10 K to the antenna temperature.

The mica windows have less than .7% reflection and add less than 1 K when clean and dry. When moistened by condensation they can contribute 20 K.

4. JPL Cooled Switch

The switch is a circulator, similar to the circulators in the maser except the magnetic field is supplied by an electromagnet rather than permanent magnets. The circulator admits radiation from one horn or the other, depending on the current in the electromagnet. On each of the three ports there is a stepped transition to a reduced height waveguide (.078"). When a magnetic field is applied to the ferrite cylinder at the center, the incoming wave turns to the right or left depending on the sign of the magnetic field. Two bits of alumina (dielectric constant 10) at each input improve the match. The measured reflection is .5% when the coil current is adjusted to give the least cross coupling between the ports (.5%). The resistivity of the titanium walls accounts for almost all of the attenuation (15%) in the switch. The switch is at 4 K so the added antenna temperature is 1 K.

5. Receiver

The bandpass filter (f1 in Fig. 1) passes 23 to 27 GHz. Its transmission at the pump frequency is 10^{-9} . Since it follows the maser its contribution to the system noise is negligible.

The mixer and LO mix the signal down to 10-410 MHz with a 5.4 dB loss. Only the upper sideband is used. A variable attenuator between the LO and the mixer was adjusted to minimize the noise of the mixer. The output is on a 50 coaxial cable. The noise temperature of the mixer is 1400 K (single sideband) or 3 K when referred to the antenna.

The IF amplifier has 54 db gain from 10 to 500 MHz. The mixer, LO, IF amplifier and detector were shielded in a copper and aluminum box. The box was in thermal contact with 1 liter of freezing water, which kept the temperature within 1 K of 273 K over the duration of the 1980 December flight. The 1981 June flight started with warm water which did not freeze until near the end of the flight. The noise temperature of the IF amplifier is about 300 K or 3 K referred to the antenna.

The detector is a tunnel diode. Noise from the diode is equivalent to a 50Ω resistor after detection. This noise and the front-end noise of the following op-amp add about $.5 \text{ mK}/\sqrt{\text{Hz}}$, or the equivalent of 10 K at the antenna, which must be added in quadrature to the other system noise. The system is summarized in Table 1.

Following the detector the switched signal is amplified with an adjustable gain amplifier which was followed by a lockin amplifier and a low pass filter. Finally the data is digitized and relayed to the ground.

II. Theoretical and Actual System Performance

The radiometer system performance is summarized in Table 1, where the calculated (or measured) noise and the relevant gain (or loss) is given for each stage. In the laboratory the system noise from the switch to the detector is measured to be 16 K, in good agreement with 16 K estimated from Table 1.

The predicted in-flight noise of 33 K can be used to calculate ΔT_{rms} Theory which can be compared to measured values. (T in this case is the difference in antenna temperatures in the two horns.)

Table 1 Source of Noise in System

	Gain (dB)	Noise (K)	Antenna Noise
Sky	-	3	3
Horns	-.09	3	3
Transition	-.04	2	2
Waveguide	-.2	8	8
Window	-.01	-	-
Switch	-.6	1	1
Maser	28	6	8
Mixer	-5.4	1400	3
IFA	54	300	3
Detector			10 (added by quadrature)
System			33 K

The noise equation for this radiometer is

$$\Delta T_{rms} \text{ Theory} = 2.2 \frac{T_{system}}{(B.W.)^{\frac{1}{2}}} \text{ K}/\sqrt{\text{Hz}} .$$

One factor of $\sqrt{2}$ comes from the 50% duty cycle of the Dicke switch; another $\sqrt{2}$ comes from the fact that the error refers to the difference in two uncorrelated temperatures. The noise is increased another 10% by

blanking of the signal at transition times of the Dicke switch. For an effective bandwidth of 300 MHz the equation gives

$$\Delta T_{\text{rms}})_{\text{Theory}} = 4.2 \text{ mK}/\sqrt{\text{Hz}} .$$

In using data from balloon flights to find $\Delta T_{\text{rms}})_{\text{Actual}}$ one must first correct for switch frequency leakage which contaminated the data. The lockin amplifier output filter (low pass) did not cut off fast enough to completely eliminate residual signal at the Dicke switch frequency (~2Hz in the December 1980 flight). This beat with the 4Hz sampling rate to give a slow beat of about 15 mK amplitude. Fortunately, the beat frequency was stable enough that the effect could be fit and removed from most of the data.

At times when maser gain was near optimum (~30 dB) the measured noise was

$$\Delta T_{\text{rms}})_{\text{Actual}} = 4 \text{ to } 5 \text{ mK}/\sqrt{\text{Hz}} ,$$

in excellent agreement with the theoretical value.

III. Data Analysis and Limitations

Data analysis is still underway at Princeton, so this report can only summarize work done so far, and anticipate where limitations in accuracy will come.

1. Preliminary Work

The data tapes from NSBF had many problems - telemetry dropout, missing time code, missing position data and occasional scrambling of data within a record. These problems were fixed at great effort and cost, and about 10% of the data were irretrievably lost. Then the switch frequency effect (see above) was fitted and removed, and the radiometer data calibrated into antenna temperature (mK). Finally balloon position and orientation and sidereal time were used to associate each radiometer reading with two positions in the sky (90° apart). From this data set a sky map can be made, or a sky model can be fit directly to the data stream. Both are done.

The usual model fit includes celestial dipole and quadrupole distributions and a model of Galactic radiation at 24.6 GHz. The Galactic radiation model includes "point" sources (mostly H II regions and supernovae remnants), free-free emission (mostly from the Galactic plane) and synchrotron radiation extrapolated from long wavelength maps. The free-free emission is estimated from H α surveys of the plane and high frequency ($\nu > 5$ GHz) surveys wherever they exist. The H α maps suffer from extinction, so are lower limits only, and the high frequency maps are incomplete. So, the free-free map is not very good. The synchrotron map must be extrapolated from 0.408 GHz to 24.6 GHz, so the spectral index (~2.80) must be known to $\sim \pm 0.05$. No one knows what the appropriate spectral index is, or how it varies over the sky.

At this point we believe that uncertainties in the Galactic radiation model will be the main limitation on finding coefficients for the celestial dipole and quadrupole components. Since Galactic radiation is strongest near the plane, we have tried cutting out data from $|b| < 10^\circ$. This will probably give the most reliable results, but the analysis is still underway.

ORIGINAL PAGE IS
OF POOR QUALITY

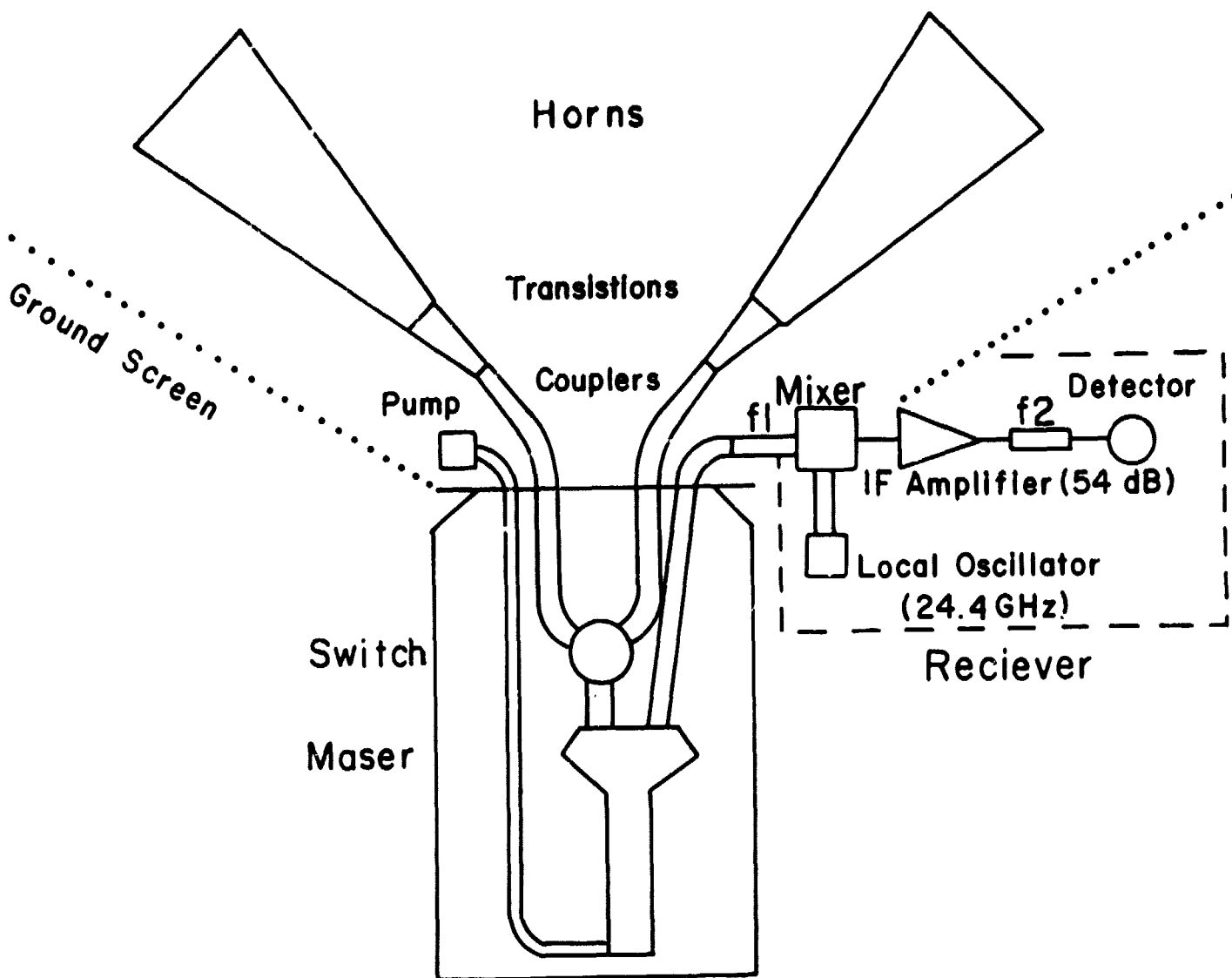


Figure 1.

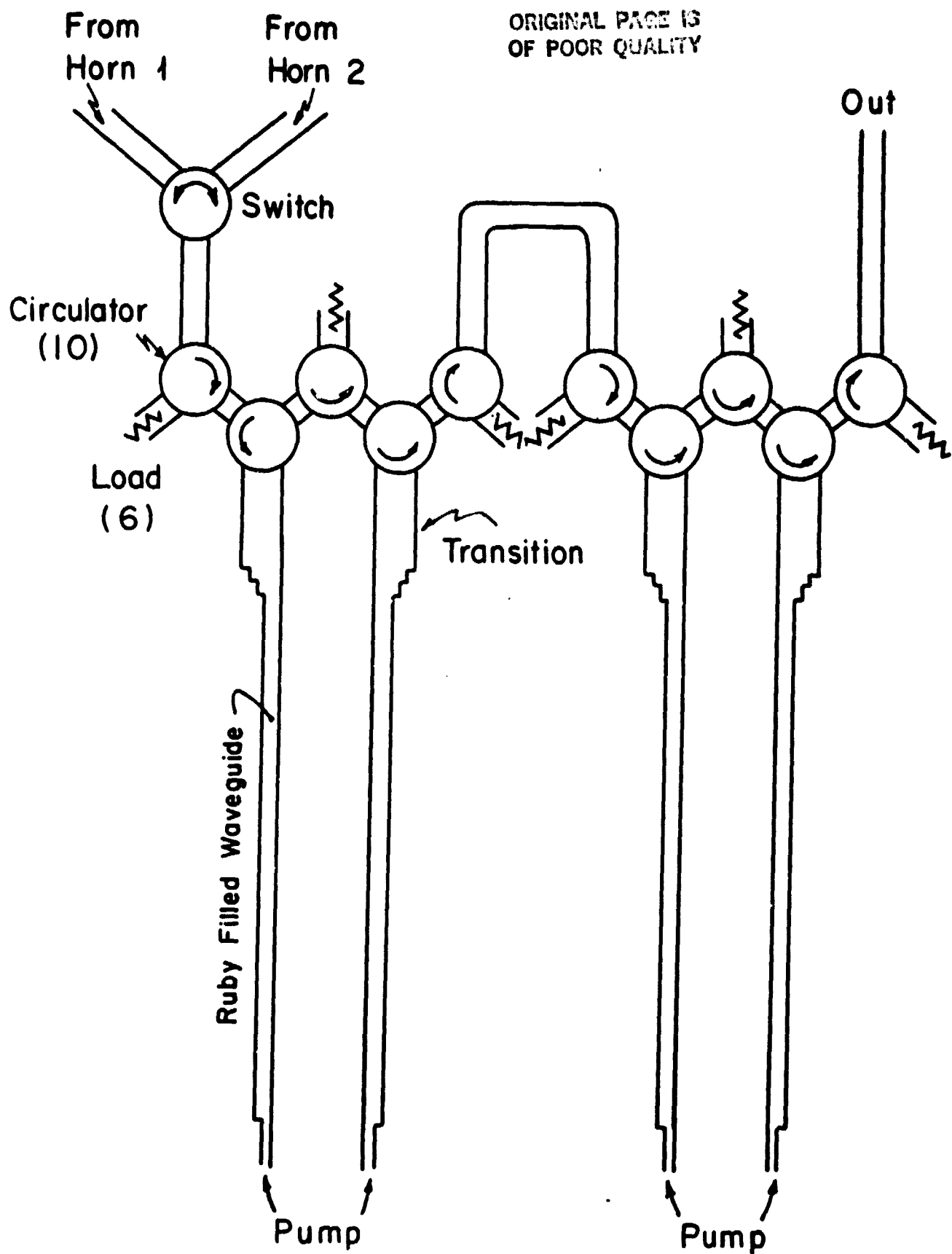


Figure 2.

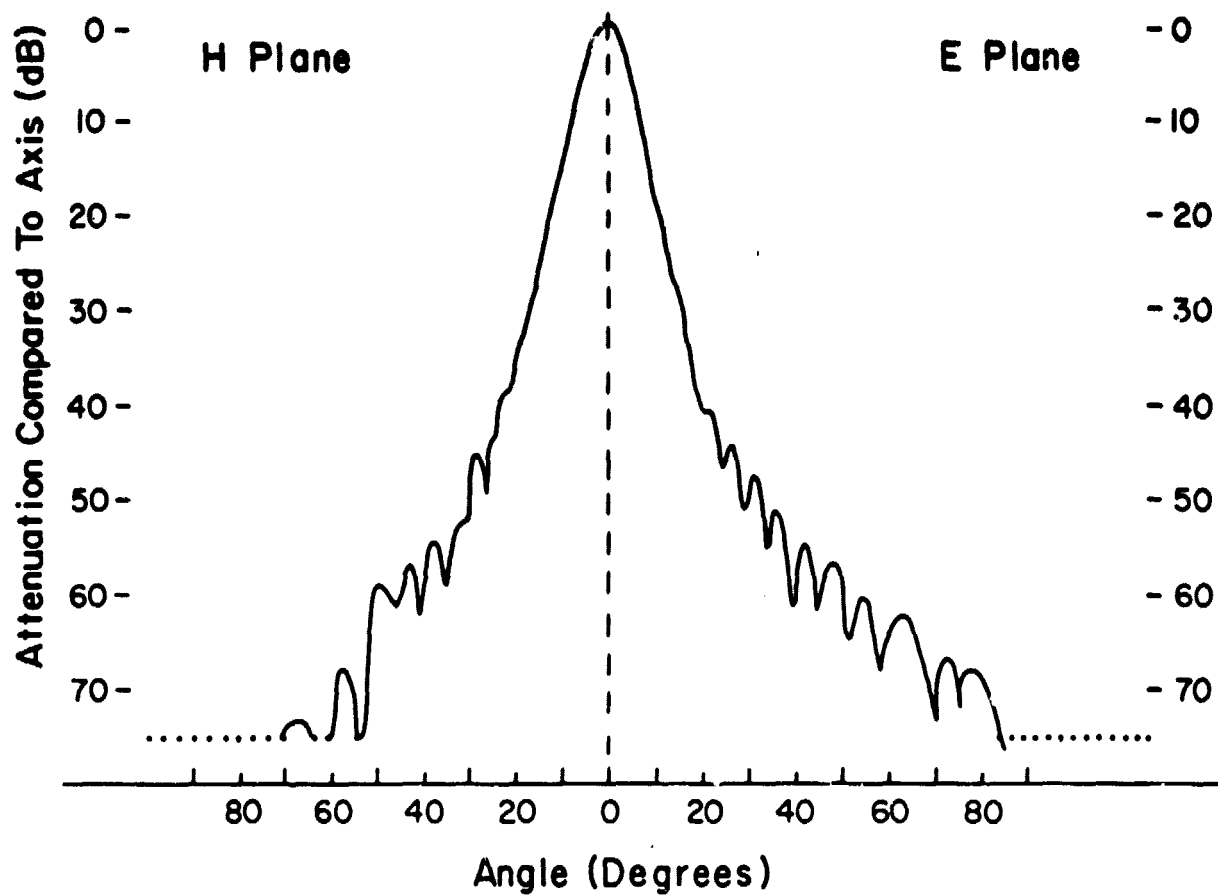


Figure 3.

Graph of Attenuation
of Power Output